Parallel determination of absolute distances to multiple targets by time-of-flight measurement using femtosecond light pulses

Seongheum Han,[1] Young-Jin Kim[2,3] and Seung-Woo Kim,[1,*]

[1]*Department of Mechanical Engineering, Korea Advanced Institute of Science and Technology (KAIST), Science Town, Daejeon, 305-701, South Korea*

[2]*School of Mechanical and Aerospace Engineering, Nanyang Technological University (NTU), 50 Nanyang Avenue, Singapore*

[3]*yj.kim@ntu.edu.sg*

[*]*swk@kaist.ac.kr*

Abstract: Distances to multiple targets are measured simultaneously using a single femtosecond pulse laser split through a diffractive optical element. Pulse arrival from each target is detected by means of balanced cross-correlation of second harmonics generated using a PPKTP crystal. Time-of-flight of each returning pulse is counted by dual-comb interferometry with 0.01 ps timing resolution at a 2 kHz update rate. This multi-target ranging capability is demonstrated by performing multi-degree of freedom (m-DOF) sensing of a rigid-body motion simulating a satellite operating in orbit. This method is applicable to diverse terrestrial and space applications requiring concurrent multiple distance measurements with high precision.

OCIS codes: (120.0120) Instrumentation, measurement, and metrology; (120.3180) Interferometry; (120.3930) Metrological instrumentation; (320.7090) Ultrafast lasers.

References and links

1. C. Fridlund, "Darwin – The Infrared Space Interferometry Mission," ESA Bull. **103**, 20–25 (2000).
2. ESA, "XEUS: X-ray evolving-universe spectroscopy," ESACDF Study Report **CDF- 31(A)**, 1–237 (2004).
3. J. Dale, B. Hughes, A. J. Lancaster, A. J. Lewis, A. J. H. Reichold, and M. S. Warden, "Multi-channel absolute distance measurement system with sub ppm-accuracy and 20 m range using frequency scanning interferometry and gas absorption cells," Opt. Express **22**(20), 24869–24893 (2014).
4. J. Mayr, J. Jedrzejewski, E. Uhlmann, M. Donmez, W. Knapp, F. Härtig, K. Wendt, T. Moriwaki, P. Shore, R. Schmitt, C. Brecher, T. Würz, and K. Wegener, "Thermal issues in machine tools," CIRP Ann.-Manuf. Technol. **61**(2), 771–791 (2012).
5. F.-J. Shiou and M.-X. Liu, "Development of a novel scattered triangulation laser probe with six linear charge-coupled devices (CCDs)," Opt. Lasers Eng. **47**(1), 7–18 (2009).
6. S.-W. Kim, H.-G. Rhee, and J.-Y. Chu, "Volumetric phase-measuring interferometer for three-dimensional coordinate metrology," Precis. Eng. **27**(2), 205–215 (2003).
7. D. Zhang, S. Rolt, and P. Maropoulos, "Modelling and optimization of novel laser multilateration schemes for high-precision applications," Meas. Sci. Technol. **16**(12), 2541–2547 (2005).
8. K. Creath, "Phase-measurement interferometry techniques," *in Progress in Optics*, E. Wolf, ed. **26**, 351–391. (Elsevier, 1988).
9. I. Fujima, S. Iwasaki, and K. Seta, "High-resolution distance meter using optical intensity modulation at 28 GHz," Meas. Sci. Technol. **9**(7), 1049–1052 (1998).
10. E. Strzelecki, D. Cohen, and L. Coldren, "Investigation of tunable single frequency diode lasers for sensor applications," J. Lightwave Technol. **6**(10), 1610–1618 (1988).
11. S.-W. Kim, "Metrology: Combs rule," Nat. Photonics **3**(6), 313–314 (2009).
12. S. Diddams, "The evolving optical frequency comb," J. Opt. Soc. Am. B **27**(11), B51–B62 (2010).
13. N. Newbury, "Searching for applications with a fine-tooth comb," Nat. Photonics **5**(4), 186–188 (2011).
14. K. Minoshima and H. Matsumoto, "High-accuracy measurement of 240-m distance in an optical tunnel by use of a compact femtosecond laser," Appl. Opt. **39**(30), 5512–5517 (2000).
15. Y.-S. Jang, K. Lee, S. Han, J. Lee, Y.-J. Kim, and S.-W. Kim, "Absolute distance measurement with extension of nonambiguity range using the frequency comb of a femtosecond laser," Opt. Eng. **53**(12), 122403 (2014).
16. J. Ye, "Absolute measurement of a long, arbitrary distance to less than an optical fringe," Opt. Lett. **29**(10), 1153–1155 (2004).

#246691 Received 24 Jul 2015; revised 16 Sep 2015; accepted 17 Sep 2015; published 23 Sep 2015

17. K.-N. Joo and S.-W. Kim, "Absolute distance measurement by dispersive interferometry using a femtosecond pulse laser," Opt. Express **14**(13), 5954–5960 (2006).
18. I. Coddington, W. Swann, L. Nenadovic, and N. Newbury, "Rapid and precise absolute distance measurements at long range," Nat. Photonics **3**(6), 351–356 (2009).
19. J. Lee, S. Han, K. Lee, E. Bae, S. Kim, S. Lee, S.-W. Kim, and Y.-J. Kim, "Absolute distance measurement by dual-comb interferometry with adjustable synthetic wavelength," Meas. Sci. Technol. **24**(4), 045201 (2013).
20. G. Wu, Q. Zhou, L. Shen, K. Ni, X. Zeng, and Y. Li, "Experimental optimization of the repetition rate difference in dual-comb ranging system," Appl. Phys. Express **7**(10), 106602 (2014).
21. J. Jin, Y.-J. Kim, Y. Kim, S.-W. Kim, and C.-S. Kang, "Absolute length calibration of gauge blocks using optical comb of a femtosecond pulse laser," Opt. Express **14**(13), 5968–5974 (2006).
22. S. Hyun, Y.-J. Kim, Y. Kim, J. Jin, and S.-W. Kim, "Absolute length measurement with the frequency comb of a femtosecond laser," Meas. Sci. Technol. **20**(9), 095302 (2009).
23. G. Wang, Y.-S. Jang, S. Hyun, B. J. Chun, H. J. Kang, S. Yan, S.-W. Kim, and Y.-J. Kim, "Absolute positioning by multi-wavelength interferometry referenced to the frequency comb of a femtosecond laser," Opt. Express **23**(7), 9121–9129 (2015).
24. J. Lee, Y.-J. Kim, K. Lee, S. Lee, and S.-W. Kim, "Time-of-flight measurement with femtosecond light pulses," Nat. Photonics **4**(10), 716–720 (2010).
25. J. Lee, K. Lee, S. Lee, S.-W. Kim, and Y.-J. Kim, "High precision laser ranging by time-of-flight measurement of femtosecond pulses," Meas. Sci. Technol. **23**(6), 065203 (2012).
26. H. Zhang, H. Wei, X. Wu, H. Yang, and Y. Li, "Absolute distance measurement by dual-comb nonlinear asynchronous optical sampling," Opt. Express **22**(6), 6597–6604 (2014).
27. H. Shi, Y. Song, F. Liang, L. Xu, M. Hu, and C. Wang, "Effect of timing jitter on time-of-flight distance measurements using dual femtosecond lasers," Opt. Express **23**(11), 14057–14069 (2015).
28. ISO, "Guide to the expression of uncertainty in measurement (GUM 1995)," ISO/IEC Guide 98–3 (2008).

1. Introduction

Multi-degree of freedom (multi-DOF) sensing of an object in 3-D space is intended to identify its location as well as orientation simultaneously with respect to a unified reference frame. Such multi-DOF sensing is essential for diverse tasks such as attitude control of satellites in orbit [1,2], beam-line alignment of particle accelerators [3], and thermal stabilization of large machinery [4]. In practice, multi-DOF sensing is accomplished by means of triangulation [5] or multilateration [6,7] which employs multiple sensors so that each one measures distance or angle within a pre-set geometrical relation with others. Various sensors of diverse principles are available for the purpose, among which gravity-referenced inclinometers or gyroscopes are preferably used for angle measurements, while laser interferometers or optical time-of-flight instruments are well suited for distance measurements in free space.

Laser distance interferometers are grouped into either incremental or absolute type, depending on the non-ambiguity range (NAR) of the measured distance. Incremental interferometers basically measure distance by means of continuous accumulation of instant interferometric phases, so the NAR is limited to half the wavelength of the source laser [8]. Incremental distance measurement offers sub-wavelength resolutions but suffers difficulty with setting up the zero fiducial point with precise geometrical relation to other sensors for multi-DOF sensing. In contrast, absolute interferometers are able to determine distance with a single measurement within an extended non-ambiguity range. Absolute distance determination is achieved usually by modulating the intensity or frequency of continuous-wave lasers [9,10]. As a result, absolute interferometers provide a well-defined zero reference for multi-DOF sensing, but their measurement accuracy is relatively lesser compared to those of incremental interferometers.

In the last decade, femtosecond lasers have been investigated as a new light source for absolute distance measurement. A single femtosecond laser is able to offer a large number of evenly spaced radio-frequency harmonics or optical wavelengths, enabling absolute distance measurement beyond the capabilities of traditional lasers [11–13]. As results, quite a few advanced interferometric techniques have been demonstrated; radio-frequency synthetic wavelength interferometry [14,15], pulse to pulse cross-correlation [16], dispersive interferometry [17], dual-comb multi-heterodyne interferometry [18–20], multi-wavelength interferometry [21–23] and time-of-flight measurement using nonlinear optical cross-correlation [24,25]. These techniques pursue the common aim to achieve the sub-wavelength

#246691 Received 24 Jul 2015; revised 16 Sep 2015; accepted 17 Sep 2015; published 23 Sep 2015

precision in long-distance ranging by making use of unique time and/or frequency domain characteristics of femtosecond lasers.

In this study, we propose an extended scheme of absolute distance interferometer for multi-DOF sensing using femtosecond laser pulses. The proposed interferometer implements simultaneous time-of-flight measurements of short light pulses sent out to multiple targets from a single pulse train source. Absolute distances are determined in parallel by combining the nonlinear optical cross-correlation technique [24,25] with dual-comb interferometry [18–20] which allows for 0.01 ps pulse timing resolution at a 2 kHz update rate. The sub-picosecond timing capability leads to sub-micrometer accuracy in measuring distances up to several meters. Finally, an uncertainty analysis is conducted to systematically validate the achieved measurement accuracy in consideration of major error sources involved in the measurement.

2. Measurement method

As illustrated in Fig. 1, the measurement system proposed in this study is based on a dual-comb interferometer employing two femtosecond lasers referred to respectively as the signal laser and the local laser. The signal laser is used as the main light source of time-of-flight measurement, while the local laser of different repetition rate is needed for frequency down-conversion sampling. The signal laser is an Er-doped fiber laser (1560 nm center wavelength) emitting 90 fs duration pulses with a 10 mW average power. A diffractive optical element (DOE) (MS-354-G-Y-A, Holo-Or) is adopted such that the output beam of the signal laser is split with a separation angle of 0.73° by means of diffraction towards multiple targets of retro-reflector type. The front-surface of the DOE is coated partially reflective, which acts as the reference target mirror reflecting the pulse M_{ref} at every pulse repetition cycle as the zero-point datum of distance measurement. Every pulse emanated from the signal laser reaches multiple targets and returns as a sequence of discrete pulses; M_{ref} in front followed by other pulses M_1, M_2, … and M_n in the time domain.

The target pulse sequence is converted to an electric signal by means of nonlinear optical cross-correlation as depicted in Fig. 1. The balanced cross-correlator (BCC) installed in the receiving part of the measurement system utilizes a PPKTP (periodically poled KTP) crystal. This type-II crystal is a second harmonic (SH) generator reacting to the cross-correlation intensity between two orthogonal polarization components [24,25]. The target pulse sequence of linear polarization is fed to one direction of the PPKTP crystal, while the other orthogonal direction is aligned to take another pulse train of linear polarization emitted from the local laser. The SH signal resulting from the PPKTP crystal is separated using a dichroic mirror (DM). For balanced detection, two separate SH signals are produced with a temporal offset by reciprocating the dual-comb interference beam to pass through the PPKPT crystal twice. The SH signals are detected using a balanced photo-detector (PD) with suppression of optical and electric background noise. The BCC signal shows that each target pulse is converted to an S-shaped signal, of which the zero-crossing point designates the target location.

For experimental validation of measurement performance, four targets (M_1-M_4) were prepared at different distances of about 3 m along the first-order diffraction lines of the DOE as illustrated in Fig. 1. Target M_4 was set on an aerostatic stage, of which the position was monitored with an incremental HeNe laser interferometer for comparative evaluation of time-of-flight measurement. The received target pulse sequence was amplified to maintain a 100 mW average power for effective generation of SH signals in the balanced cross correlator (BCC). Pulse broadening due to long fiber delivery was compensated by inserting a dispersion compensating fiber so that the duration for each target pulse was kept to be ~510 fs. The repetition rate of the signal as well as the local laser was stabilized by phase-locking control to the Rb clock with a 10^{-12} stability at 1 s averaging.

#246691 Received 24 Jul 2015; revised 16 Sep 2015; accepted 17 Sep 2015; published 23 Sep 2015

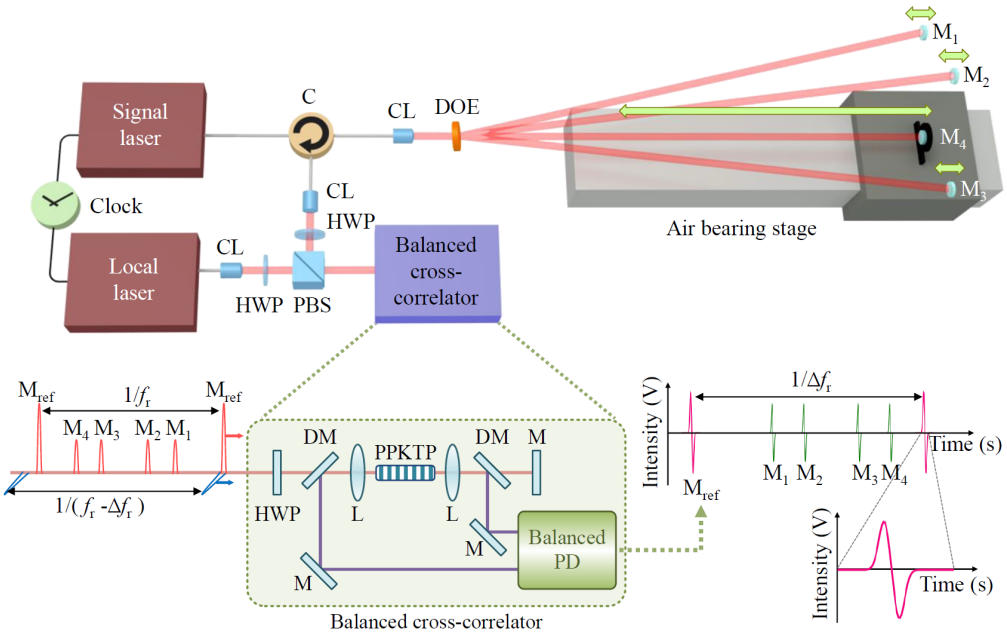

Fig. 1. Measurement system for absolute ranging to multiple targets. C: circulator, CL: collimator, DOE: diffractive optical element, HWP: half-wave plate, PBS: polarizing beam splitter, f_r: pulse repetition rate, Δf_r: repetition rate difference between the signal and local lasers, L: lens, M: target mirror, PD: photo-detector, DM: dichroic mirror, and PPKTP: periodically poled KTP crystal.

The distance d to each target is determined as $d = c\Delta t/(2N)$ with c being the vacuum speed of light, N the group refractive index of air, and Δt the time-of-flight of the pulse for return travel between the DOE and the target. Time-of-flight Δt may be measured directly in the real time domain by counting the elapse time of each target pulse using relevant electronic instruments, but this conventional way of pulse timing offers no benefit of using femtosecond pulses. This is because even state-of-the-art photodetectors are still not fast enough to resolve femtosecond pulses, thus the timing resolution remains a few picoseconds at best, equivalent to several hundreds of micrometers in distance. Instead, the BCC scheme of Fig. 1 combined with dual-comb interferometry is able to enhance the timing resolution and also accuracy of time-of-flight measurement intended using femtosecond pulses. For dual-comb interferometry, the signal laser is operated at a repetition rate of f_r, and the local laser is set to a slightly different repetition rate with an offset of Δf_r from f_r. Then, collective beating of all the optical modes in dual-comb interferometry makes the BCC signal repeat at Δf_r, permitting detection of the time-of-flight Δt in a slowed time scale down-converted by the factor of $f_r/\Delta f_r$ [26,27].

In our experiment, Δf_r was set at 2 kHz while f_r was 100 MHz with the ratio $f_r/\Delta f_r$ being 5×10^4. Figure 2(a) shows an actual BCC signal which was digitized at a fast sampling rate (f_s) of 200 MHz using a 14 bit digitizer so as to minimize quantization error [20]. A low-pass filter with a cutoff frequency of 35 MHz was incorporated to suppress both the repetition rate signals of f_r and f_r-Δf_r and also unwanted high frequency noise. The sampled BCC signal is displayed in the 'effective time' scale by up-converting the sampling rate as $f_s' = f_s \times (f_r/\Delta f_r)$ with the effective sampling rate f_s' being worked out to be 10.0 THz. This infers that the sampling resolution in the effective time scale is equivalent to 0.1 ps. Now, the time-of-flight Δt is quantified by locating the zero-crossing point of the S-shaped BCC pulse signal from its cross-correlation with a standard BCC signal pattern (Fig. 2(b)). The peak location of the resulting cross-correlation curve (Fig. 2(c) and 2(d)) is recognized as the zero-crossing

#246691 Received 24 Jul 2015; revised 16 Sep 2015; accepted 17 Sep 2015; published 23 Sep 2015

position. This electronic signal processing leads to a drastic improvement in the pulse timing resolution of determining Δt, far better than the pulse sampling resolution of 0.1 ps, which will be discussed in detail with experimental results in the next section.

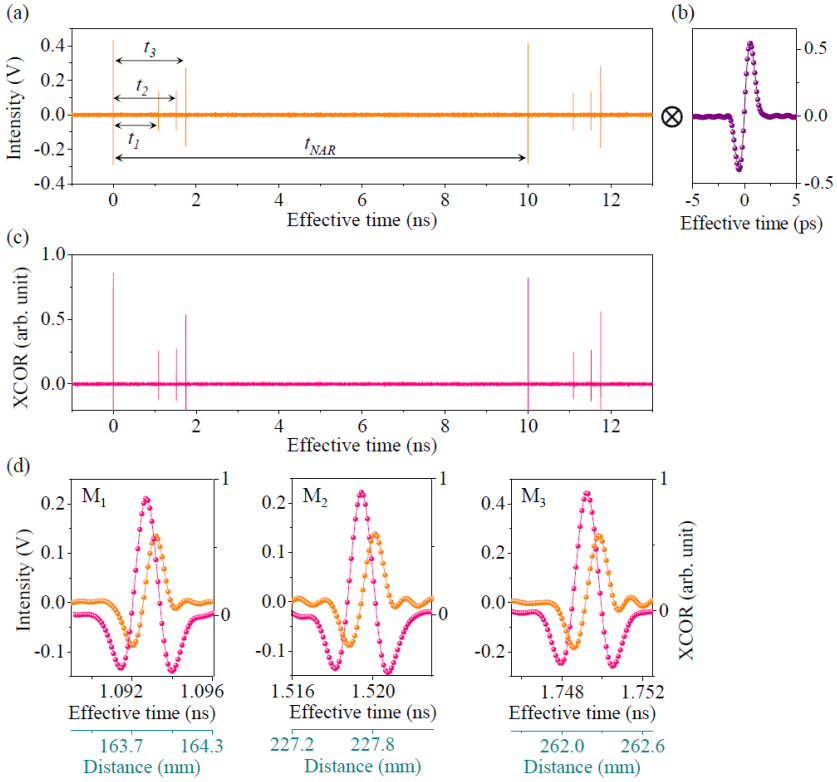

Fig. 2. BCC signal sampling and cross-correlation processing. (a) An exemplary BCC signal sampled from three targets. (b) Reference BCC signal pattern for cross-correlation. (c) Cross-correlation between the reference and the measurement BCC signal. (d) Enlarged views of cross-correlation curves for peak detection. Yellow lines indicate original sampled BCC signals and red curves are calculated cross-correlation data.

3. Performance evaluation

Figure 3 shows experimental results obtained to evaluate the repeatability, linearity and speed of the measurement system described so far. During the experiment, the environmental condition was controlled by regulating the ambient temperature, pressure, humidity and CO_2 concentration as listed in Table 1. Firstly, the measurement repeatability was observed in terms of the Allan deviation for two distances selected at d_1 = 0.015 m and d_2 = 1.6 m (Fig. 3(a)). Note that the Allan deviation was given as a function of the averaging time, of which the shortest time was 0.5 ms corresponding to a single measurement time as the distance reading was updated at 2 kHz rate. Figure 3(a) shows that the repeatability for d_1 was 0.936 μm for 0.5 ms averaging. The single-measurement repeatability lies below 0.01 ps which is in fact one order of magnitude less than the sampling resolution of 0.1 ps. The repeatability improves further to 17 nm for 0.5 s averaging, of which the timing resolution reaches the range of 0.1 fs with increased averaging to cover 1,000 distance readings. It is worthwhile to note that the test distance d_1 is short enough to neglect the effects of external disturbance such as vibration, temperature variation and air fluctuation. In other words, the repeatability for d_1 can be considered as the standard uncertainty (k = 1) of the measured time-of-flight Δt itself.

#246691 Received 24 Jul 2015; revised 16 Sep 2015; accepted 17 Sep 2015; published 23 Sep 2015

As such, the repeatability for d_2, which is longer than d_1, appeared to be worse than that of d_1, regardless of the averaging time, being attributed to increased external disturbance.

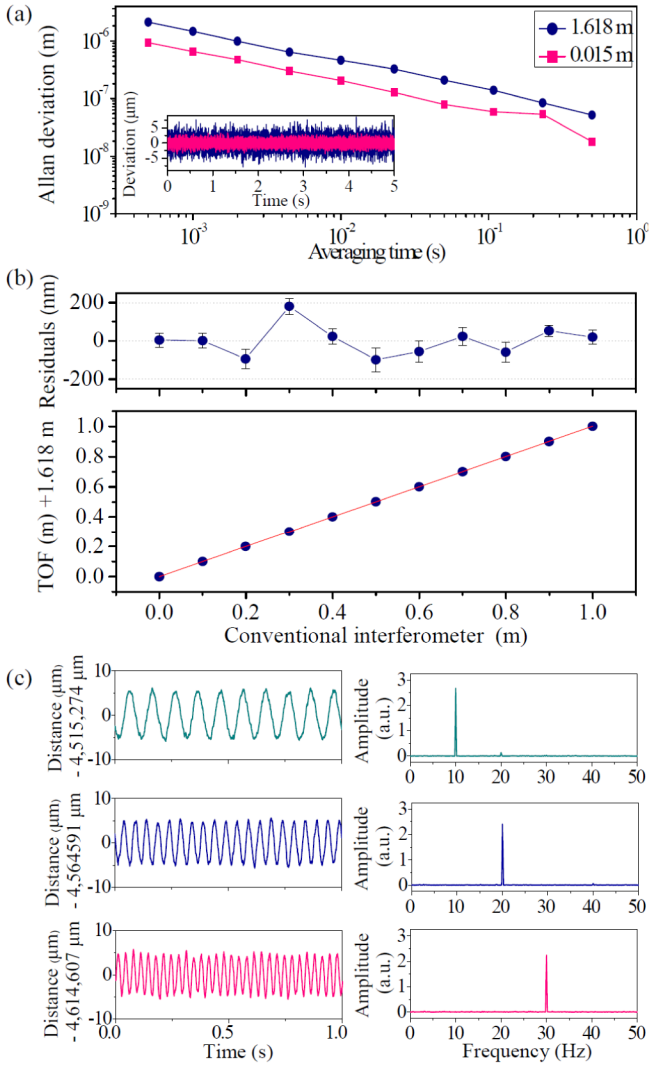

Fig. 3. Absolute multi-target ranging performance. (a) Repeatability in Allan deviation at two distances. (b) Linearity test result compared with an incremental HeNe laser interferometer. (c) Speed of absolute ranging of multiple target objects. Three targets were modulated at 10, 20 and 30 Hz, respectively, using PZTs. During all the tests, the environment was controlled as specified in Table 1 in terms of temperature, pressure, humidity and CO_2 concentration.

Secondly, the linearity test of the measurement system was conducted in comparison with an incremental HeNe laser interferometer. The target mirror of M_4 in Fig. 1 was moved over a 1.0 m travel, from 1.6 m to 2.6 m in distance, on an aerostatic stage in 100 mm steps (Fig. 3(b)). The maximum deviation between the two measurements was 279 nm at 0.5 s averaging (79 nm in standard deviation), while no cyclic error was observed. Thirdly, the distances to three targets of M_1, M_2 and M_3 of Fig. 1 were modulated with a same ~10 μm amplitude but with different frequencies of 10, 20, and 30 Hz, respectively, using piezoelectric actuators (PZTs) installed underneath the targets to provide dynamic distance variations. As shown in Fig. 3(c), the sinusoidal motions of three targets were precisely monitored and reconstructed;

#246691 Received 24 Jul 2015; revised 16 Sep 2015; accepted 17 Sep 2015; published 23 Sep 2015

Fourier analysis confirmed that absolute distances to multiple targets are clearly resolved with a high signal-to-noise ratio in the frequency domain.

4. Multi-DOF sensing

Multi-DOF sensing capability of our measurement system was tested with an experimental apparatus configured with a rigid body simulating the satellite motion as illustrated in Fig. 4. Four target mirrors M_1-M_4 were installed on the rigid body with a 90 degree apart along the ± 1st-order diffraction lines of the DOE. The mirrors were positioned with a ~1.0 mm distance offset from each other, so they can be distinguished by the pulse arrival order in the BCC signal. On the rigid body, the local *xyz*-coordinates are set up so that the *x*-axis connects M_1 and M_3 while the *y*-axis is aligned from M_2 to M_4. The normal vector was set along the *z*-axis at the origin of the *xy* plane, of which the orientation was defined by the yaw angle θ_x and the pitch angle θ_y with respect to the 0th-order diffraction line of the DOE. Let d_1, d_2, d_3, and d_4 be the distances measured to the target mirrors from the DOE, then the nominal distance d to the rigid body is calculated by the mean of the four measured distances; $d = (d_1 + d_2 + d_3 + d_4)/4$. At the same time, the yaw and pitch angles are calculated instantly as $\theta_x = \sin^{-1}[(d_1 - d_3)/A]$ and $\theta_y = \sin^{-1}[(d_2 - d_4)/A]$.

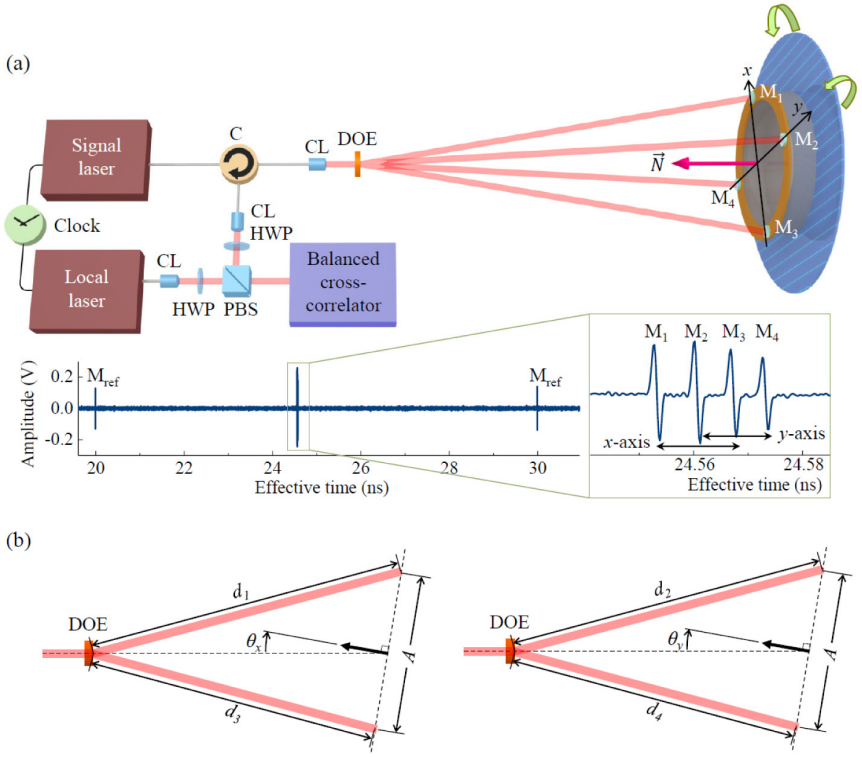

Fig. 4. Distance and angle measurement for multi-DOF sensing of a rigid body motion. (a) Experimental configuration. (b) Measurement geometry. C: circulator, CL: collimator, DOE: diffractive optical element, PBS: polarizing beam splitter, and HWP: half wave plate.

Figure 5 shows a repeatability result for angular motions obtained for the rigid body located at a nominal distance of ~3.7 m. When the rigid body was stationary, the Allan deviation was 5.289 arcsec at 0.5 ms averaging, decreasing further to 0.073 arcsec with increasing the averaging time to 0.5 s. Next, for testing of dynamic measurements, the rigid body was given continuous tilt motions modulated at 1 Hz excitation using PZTs with different modulation amplitudes. Four distances (d_1, d_2, d_3, and d_4) were measured, from

#246691 Received 24 Jul 2015; revised 16 Sep 2015; accepted 17 Sep 2015; published 23 Sep 2015

which yaw and pitch angles were calculated. Fourier-transformed signals clearly showed individual modulation peaks at 1 Hz with different amplitudes for yaw and pitch angles. Note that 2nd and 3rd harmonic peaks due to imperfect excitation were also observed at 2 Hz and 3 Hz.

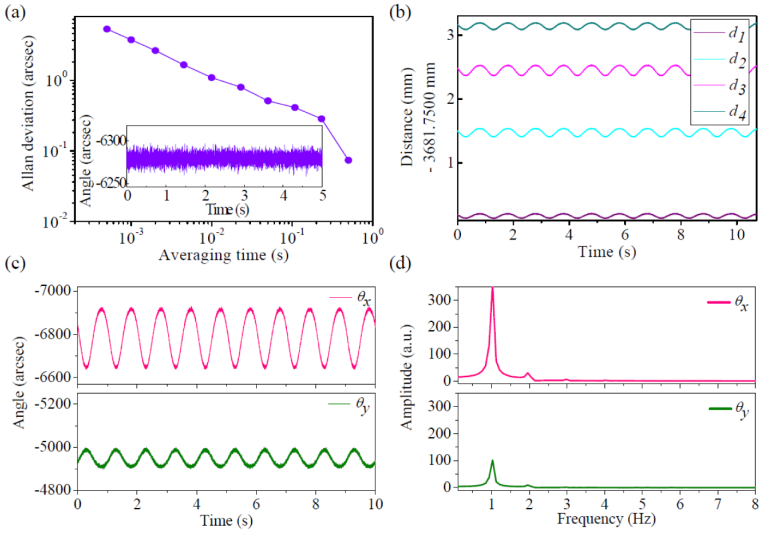

Fig. 5. Angle measurement test result. (a) Repeatability in terms of Allan deviation. (b) Distances (d_1, d_2, d_3, and d_4) to four targets under 1 Hz excitation. (c) Reconstructed angular motions. (d) Fourier transformed spectra of (c).

5. Uncertainty evaluation for absolute distance measurement

As summarized in Table 1, the measurement uncertainty was evaluated in accordance with the guideline provided by the international organization for standardization (ISO) [28]. Our systematic analysis starts with the target distance expressed as

$$d = m\Lambda + \frac{c\Delta t}{2N} \tag{1}$$

where m is an integer (m = 0, 1, 2, …) and Λ denotes the non-ambiguity range (NAR) given by $\Lambda = c/(2f_{\mathrm{r}}N)$. Equation (1) indicates that there are four major uncertainty sources; the timing accuracy Δt, the signal laser repetition rate f_{r}, the repetition rate offset Δf_{r} and the group refractive index of air N. The combined standard uncertainty $u_{\mathrm{c}}(d)$ is defined as

$$u_{\mathrm{c}}(d) = [c_{\Delta t}^2 u^2(\Delta t) + c_{f_{\mathrm{r}}}^2 u^2(f_{\mathrm{r}}) + c_{\Delta f_{\mathrm{r}}}^2 u^2(\Delta f_{\mathrm{r}}) + c_N^2 u_{\mathrm{c}}^2(N)]^{1/2} \tag{2}$$

with sensitivity coefficients; $c_{\Delta t} = \partial d/\partial \Delta t$, $c_{\mathrm{fr}} = \partial d/\partial f_{\mathrm{r}}$, $c_{\Delta \mathrm{fr}} = \partial d/\partial \Delta f_{\mathrm{r}}$, and $c_N = \partial d/\partial N$. The standard uncertainty of each source (k = 1) is determined based on relevant experimental data. First, the uncertainty for Δt was estimated from the result of Fig. 3(a) obtained at a 0.015 m distance, which is worked out to be $u(\Delta t) = 1.1 \times 10^{-16}$ s, corresponding to 17 nm in distance. Second, the uncertainty for f_{r} was 3.7×10^{-12} d with d being the nominal distance given in meter, which was estimated from the Allan deviation at 0.5 s averaging. Being in proportion to d, this uncertainty contribution becomes significant for long distances. Third, the uncertainty for Δf_{r} originates from the relative phase jitter between the signal laser and the local laser. This contribution appears to be dominant for short distances because the timing jitter is amplified by the factor of $f_{\mathrm{r}}/\Delta f_{\mathrm{r}}$ in the effective time scale. The uncertainty for repetition rate offset Δf_{r} is estimated at 0.5 s averaging to be 188 nm. Fourth, the uncertainty for N is estimated to be 1.8×10^{-8} d, in consideration of the uncertainty of the empirical

#246691 Received 24 Jul 2015; revised 16 Sep 2015; accepted 17 Sep 2015; published 23 Sep 2015

Ciddor's equation as well as the environmental parameters of temperature, pressure, relative humidity, and CO_2 concentration. Finally, the combined uncertainty is worked out to be $[(1.7 \times 10^{-8}\, d)^2 + (189\ \text{nm})^2]^{1/2}$ for the nominal distance d. The uncertainty evaluation result reveals that the repetition rate offset Δf_r turns out to be the most influencing uncertainty source for absolute ranging within a few meters. For longer distances, the air refractive index becomes significant. It should be noted that the uncertainty evaluation presented in Table 1 was based on the experimental data obtained at 0.5 s averaging time in a well-controlled environmental condition. The uncertainty level can be enhanced by increasing the averaging time to an extent where the atomic clock provides better accuracy for stabilizing Δf_r. However, in reality, the ultimate limit in achieving high level of combined uncertainty is imposed by the refractive index of air particularly for long distances to be measured in open air conditions.

Table 1. Uncertainty evaluation of distance measurement.

Uncertainty source, x_i	Standard uncertainty, $u(x_i)$	Sensitivity coefficient, $\lvert c_{xi}\rvert$	Contribution of $\lvert c_{xi}\rvert u(x_i)$ for d
Time-of-flight measurement, (0.5 s averaging)			$[(3.7 \times 10^{-12}\, d)^2 + (189\ \text{nm})^2]^{1/2}$
Timing accuracy, Δt	1.1×10^{-16} s	1.5×10^{8} m·Hz	17 nm
Repetition rate (signal laser), f_r	3.7×10^{-4} Hz	1.0×10^{-8} Hz^{-1} d	3.7×10^{-12} d
Repetition rate offset, Δf_r	2.5×10^{-4} Hz	7.5×10^{-4} m·s	188 nm
Refractive index of air (group), N			1.7×10^{-8} d
Ciddor's equation	1.0×10^{-8}	d	1.0×10^{-8} d
Temperature	5.8 mK	9.2×10^{-7} d/K	5.3×10^{-9} d
Pressure	3.0 Pa	2.7×10^{-9} d/Pa	8.1×10^{-9} d
Relative humidity	1.0%	8.7×10^{-9} d/%	8.7×10^{-9} d
CO_2 content	39 ppm	1.4×10^{-10} d/ppm	5.5×10^{-9} d
Combined standard uncertainty (k = 1) (In the case of d = 1.618 m)			$[(1.7 \times 10^{-8}\, d)^2 + (189\ \text{nm})^2]^{1/2}$ (189 nm)

6. Conclusions

Parallel determination of absolute distances to multiple targets was demonstrated by time-of-flight measurement using femtosecond light pulses. The timing resolution was 0.01 ps at a 2 kHz update rate, which was attained by combining the principle of dual-comb interferometry with nonlinear balanced cross-correlation of time-of-flight measurement. This sub-ps multi-target ranging capability was tested by performing multi-degree of freedom sensing of a rigid-body object simulating a satellite operating in orbit. The ranging repeatability was 17 nm in terms of the Allan deviation at 0.5 s averaging, while a 0.073 arcsec repeatability was obtained for angle measurement. This result is in agreement with the uncertainty analysis conducted in consideration of all dominant error contributions. This method has the potential for diverse terrestrial and space applications requiring concurrent multiple distance and angle measurements.

Acknowledgments

This work was supported by the National Honor Scientist Program funded by the National Research Foundation of the Republic of Korea (NRF-2012R1A3A1050386). Y.-J. Kim acknowledges support from the Singapore National Research Foundation (NRF-NRFF2015-02) and thanks N. R. Newbury, I. Coddington, and W. C. Swann at the National Institute of Standards and Technology (NIST) for fruitful discussions and technological supports.

#246691 Received 24 Jul 2015; revised 16 Sep 2015; accepted 17 Sep 2015; published 23 Sep 2015